Integrated optics for the characterization of photoreactive organic thin films

Wolfgang Knoll

Max-Planck-Institut für Polymerforschung, Ackermannweg 10, D - 55021 Mainz, Germany and Frontier Research Program, The Institute of Physical and Chemical Research (RIKEN), Wako, Saitama 351-01, Japan

Abstract

Integrated optical techniques are introduced as a powerful approach for the investigation of thin organic films and their photo-physical and -chemical properties. Waveguide and surface plasmon spectroscopies and microscopies are shown to sensitively monitor optical and structural modifications in these ultrathin layers upon irradiation with light.

After a short introduction into the field of evanescent- and guided wave-optics we will give various examples that are chosen so as to demonstrate where and when integrated optics offer analytical advantages over more classical techniques with plane waves, "normal" photons.

Among the photo-chemical examples discussed are studies with various types of polysilane films that volatilize upon irradiation with UV light. We compare, in particular, differences between films prepared by spin casting to those fabricated, layer by layer, by the Langmuir-Blodgett-Kuhn technique with their substantially higher internal order.

An interesting structure / property relation is found for different polymer systems functionalized by photo-isomerizing azobenzene chromophores. The systems investigated range from liquid-crystalline (LC), side group polymers in planar waveguide format to single monolayers acting as photo-responsive command layer for LC cells.

I. Integrated Optics with Surface Plasmons and Waveguide Modes

Plasmon surface polaritons ("surface plasmons" or PSP for short) are surface electromagnetic modes associated with a polarization charge wave propagating along a metal-dielectric interface. Their field amplitudes decay exponentially, both into the dielectric and into the metal, respectively, with the maximum intensity being at the interface. As can be seen from the dispersion relation which, for a flat metal surface in air or vacuum, is given by [1]

$$k_{sp}^0 = \frac{\omega}{c}\sqrt{\frac{\varepsilon_m(\omega)}{\varepsilon_m(\omega)+1}}, \tag{1}$$

with k_{sp}^0 the PSP wave vector, ω is the frequency, c the speed of light, and $\varepsilon_m(\omega) = \varepsilon_{mr}(\omega) + i\varepsilon_{mi}(\omega)$ the complex dielectric function of the metal, PSP cannot be excited directly by photons because their momentum,

$$k_{ph}^0 = (\omega / c)\sin\phi, \tag{2}$$

is too small, at any angle of incidence ϕ, for resonant coupling, i.e., for energy *and* momentum matching between photons and surface plasmons. Various coupling schemes have been proposed among which the attenuated total internal reflection (ATR) prism configuration in the Kretschmann setup [2] is the most

widespread: Basically, the momentum of the exciting photon is increased by n_0, the index of refraction of the prism, so that now coupling is possible at a well-defined angle ϕ_0, where

$$k_{sp}^0 = k_{ph}^0 = n_0(\omega/c)\sin\phi_0. \tag{3}$$

An ATR experiment scans the angle of incidence and the reflected intensity is recorded by a photodiode (see Fig. 1(a)).

Now, a thin dielectric coating causes an increase of the PSP wave vector,

$$k_{sp}^1 = k_{sp}^0 + \Delta k_{sp}, \tag{4}$$

which, according to Eq. (3), shifts the resonance to a higher angle ϕ_1. From this shift one can calculate, on the basis of Fresnel's equations, the optical thickness of the coating, i.e., the geometrical thickness provided its index of refraction n is known [3].

If the thickness of the coating is further increased, a new type of non-radiative mode, guided optical waves, can be observed. This is schematically illustrated in Fig. 1(b). Generally, these modes can be excited if the light travelling inside such a thin slab configuration is totally reflected at the boundaries to the surrounding media and fulfils the well-known mode equation [4]

$$kd + \beta_0 + \beta_1 = m\pi \tag{5}$$

with k being the wavevector of the mode of order m, d the thickness of the waveguide structure and $2\beta_i = r_i'' / r_i'$ with $r_i = r_i' + ir_i''$ the complex reflection coefficient at the interface between waveguide and metal, and waveguide and air, respectively. The excitation of these modes of different order again can be seen if the reflected intensity is recorded as a function of the angle of incidence, ϕ (Fig. 1(b), lower part): narrow dips in the reflectivity curve above ϕ_C indicate the existence of the various guided waves. For a given material combination their number and angular position only depend on the waveguide thickness. For illustration purposes we have drawn the field amplitudes of the first three modes indexed according to their number of nodes inside the waveguide: $m=1,2,3$. What makes guided optical waves a particularly
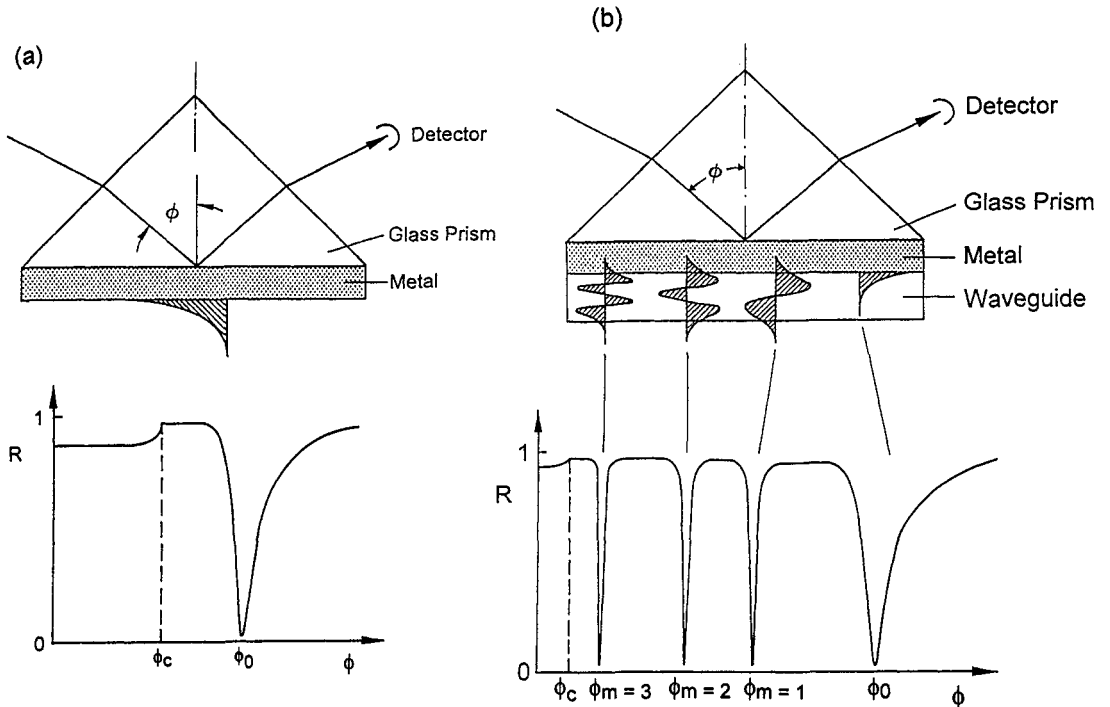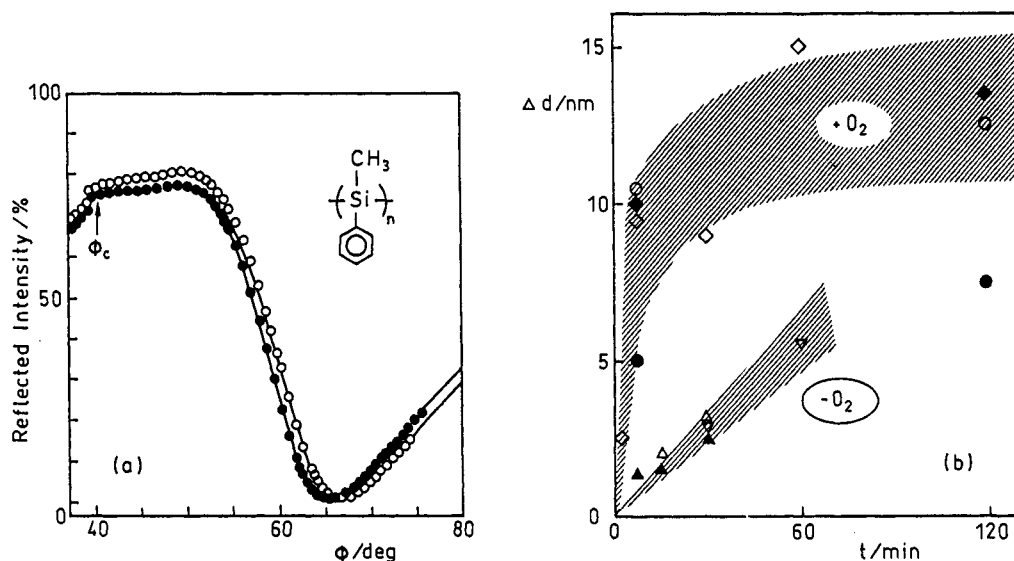

Figure 1

Figure 2

valuable diagnostic tool is the fact that they can be excited with both TM- and TE-light (TM: transverse magnetic; TE: transverse electric), i.e., with p- and s-polarized photons. For polymeric materials with optical anisotropy this means that different components of the dielectric tensor of the thin film structure can be probed.

II.   Photo-volatilization of polysilane films

One possible application of the dependence of the PSP coupling conditions to the coating thickness is the observation of the loss of film thickness by partial photo-volatilization of the coating material upon UV-irradiation [5] (Fig. 2(a)). The sample was a thin layer of poly(phenyl-methyl-silane) [6] prepared by spin-casting onto the Cr/Au-coated substrate. The starting thickness was d_0=42.5 nm as determined from the reflectivity scan. After irradiating the sample for t=7.5 min in an Ar-atmosphere with light from a low pressure mercury lamp (at a power density of ca. 1.75 mW/cm^2) the position of PSP excitation is shifted to smaller angles - a clear indication that the optical thickness was decreased. If we use the refractive index of the bulk material (n=1.635) for the Fresnel fit of the remaining film thickness we obtain d_1=41.2 nm which means that the obtained shift of the resonance is caused by the volatilization of an equivalent film thickness of only Δd=1.3 nm.

The time dependence of this etching process (see Fig. 2(b)) revealed substantial differences between irradiation in air or in an Ar-atmosphere of 10^{-3} MPa partial pressure: For 40-nm-thick films in the presence of oxygen an ablation rate of 1.3 nm/min is derived for the first 5-10 min which drops rather abruptly to zero (irradiation power density ~ 0.4 mW/cm^2). In Ar-atmosphere the etching rate is ~ 0.1 nm/min but constant for more than 1 h. These differences are discussed in terms of the different photochemical reactions following the primary Si-Si scission process induced by the UV-photon absorption.

It is interesting to compare these results obtained with amorphous, spin-cast thin films with those from highly ordered systems prepared by the Langmuir-Blodgett-Kuhn (LBK) technique. For this purpose multilayer assemblies of poly(bis-[(m)-butoxy-phenyl])silane were fabricated by multiple dipping and withdrawing of the Au-coated substrate through a monomolecular layer prepared at the water/air-interface [7]. Fig. 3 shows the reduction in thickness as a function of time for samples of 2, 6, and 20 monolayers, respectively. Clearly seen is the different ablation behavior compared to the spin-cast films. This is interpreted as being due to a reduced crosslinking tendency in these highly organized films.

The above described angular shift of the resonance condition for different coating thicknesses is also the basic mechanism that generates the high contrast achievable in surface plasmon microscopy (SPM) of heterogeneous thin films. Here, the reflected, scattered and diffracted plasmonic light is Fourier-
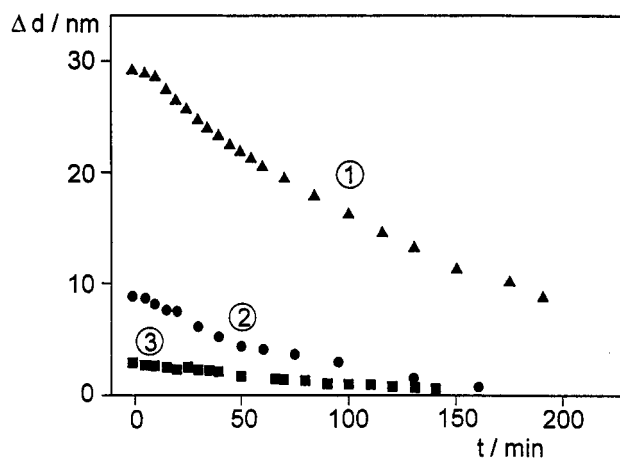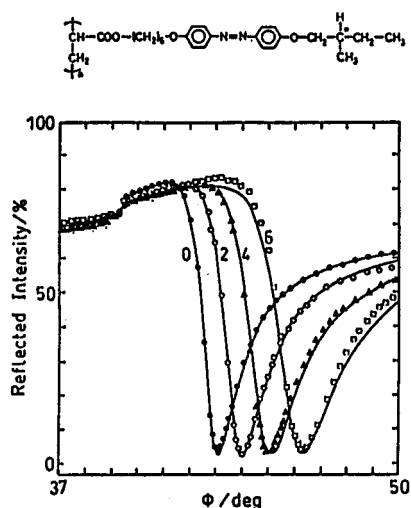
Figure 3

Figure 5

backconverted by a lens to form an image of the interface in real space on a TV-camera in our case (see Fig. 4(a)). Only those areas that are at resonance appear dark, whereas all other domains according to their relative shift of the coupling condition are more or less bright.

If a polysilane film is only partially ablated by irradiating the sample through a mask, both irradiated as well as unexposed areas can be observed right next to each other and thereby allow for a quantitative evaluation of the photoablation and photovolatilization processes. An example is given in Fig. 4(b) where a line grid had been used as a mask. Shown are SPM pictures taken at different angles of incidence ϕ, as indicated. One can see that the thinner (the exposed) areas are the first to be tuned into resonance. Between $\phi=66°$ and $\phi=67°$ the contrast inversion point is found, and then the unexposed areas are darkest before the intensity for all areas increases again and the contrast fades away (not shown). A quantitative analysis starts with a grey value histogram taken by an image-analyzing program from all pixels in a frame of about $100 \times 100 \ \mu m^2$ in the two different areas, respectively. The mean values are plotted in Fig. 4(c) (open symbols, irradiated; full symbols, unexposed) as a function of the angle of incidence of the respective picture. The obtained experimental dependence can be fitted (after proper calibration) to Fresnel calculations and yield $d_1=47.7$ nm for the unexposed (dashed curve), and $d_2=45.7$ nm for the irradiated areas (full curve).

III. Azobenzene-functionalized polymers

The investigation of the *trans↔cis* photoisomerization of azobenzene derivatives is of great interest for fundamental questions in basic research as well as for its importance in view of possible applications in optical data storage systems. In particular, if the chromophores are linked covalently to a polymeric backbone the structural properties of the resulting liquid-crystalline polymer and their coupling to the molecular configuration of the azobenzene groups are still a much debated problem in the field of matrix-dependent photophysical and photochemical processes.

In a first set of experiments, monolayers of a liquid-crystalline side-chain homopolymer bearing azobenzene derivatives as the mesogenic sidegroups [8] (structure formula given in Fig. 5) were deposited directly onto the PSP-carrying Au layer at the base of a glass prism and gave a series of angular reflectivity scans taken with the bare substrate (•), and after coating with 2, 4, and 6 layers of the polymer (Fig. 5). The full curves are calculated reflectivities based on a Fresnel simulation of the interfacial architecture that assumed a constant index of refraction $n_z=1.493$ and a constant thickness d=2.52 nm for each of the monolayers. The good agreement in Fig. 5 between measured and calculated data indicates i) the quantitative understanding of PSP excitation at these complex interfaces and ii) that the LBK deposition allows one to prepare multilayer assemblies that are, indeed, the multiple of a monomolecular basic unit.
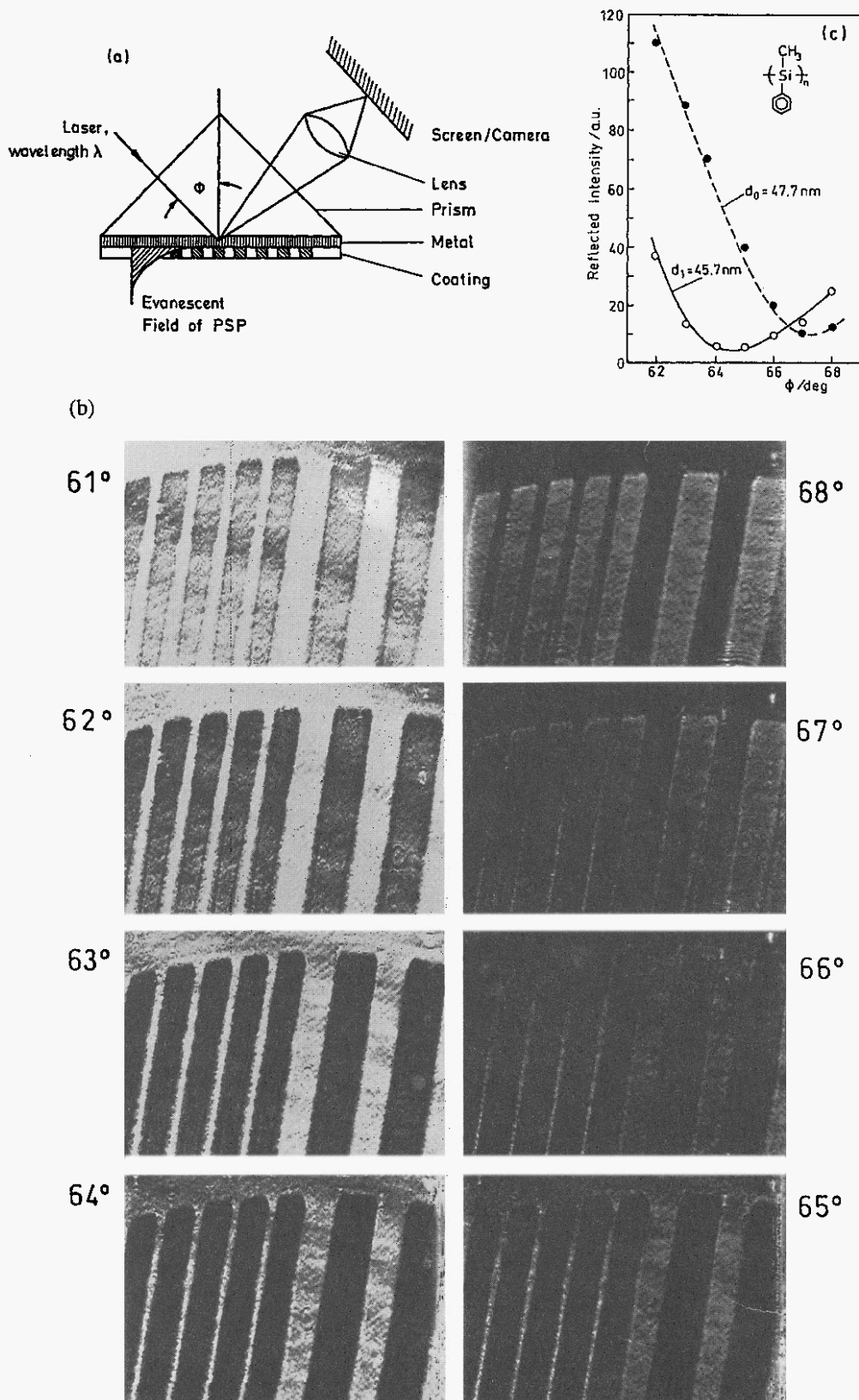
Figure 4

The next example, given in Fig. 6, describes the effect of the photo-induced trans-cis isomerization reaction in azobenzene chromophores containing side-chain copolymers, prepared as multilayer assemblies by the LBK technique [9]. The monolayers deposited were prepared from a material similar to the one used for the experiments in Fig. 5, but this time the photo-reactive units were "diluted" by mesogenic phenylbenzoate side-chains in a ratio of 1:2 (structure formula given in Fig. 6(a)). Before illumination of the multilayer assembly, prepared in the dark-adapted trans-state, a reference scan of the sample's reflectivity was taken (● in Fig. 7(a)) and evaluated to give the out-of-plane refractive index $n_z=1.567$ (knowing the sample's thickness from X-ray measurements). Irradiating the layers for t=10 min with

$\lambda=(360\pm30)$ nm light caused an angular shift of the resonant PSP excitation to smaller angles (Δ in Fig. 6(a)). This indicated that the optical thickness of the sample had decreased. However, simultaneous X-ray reflectometry measurements had shown a minor increase of the film thickness upon irradiation. Taking this into account, one then could calculate the change in the refractive index anisotropy as it is probed by surface plasmon modes as the variation of n_z with time. A rapid on-line monitoring of these changes is possible if one records the reflected intensity as a function of time at a fixed angular position (for example 47.2° as marked by the arrow in Fig. 6(a)). The linear approximation of the slope of the reflectivity curve allows for a direct transformation of the intensity change into an angular shift of the resonance and from that into the corresponding change of n_z (Fig. 6(b)).

The (partial) optical reversibility of this index change was inferred from the PSP resonance behavior monitored while the sample was illuminated with visible light ($\lambda=(450\pm30)nm$). This analysis showed the back-reaction of n_z to larger values. These illumination cycles could be repeated many times (Fig. 6(b)). Given the signal-to-noise ratio of the on-line record of the intensity variation with time, the sensitivity for measuring such, or other, photo-induced refractive index changes was estimated to be about $\Delta n/n=10^{-4}$ at a sample thickness of only $d \approx 15$ nm! This was sensitive enough to monitor the equivalent changes induced in just a single bilayer of this photo-reponsive material. The kinetic information thus obtained showed a complex behavior with a time constant distribution depending upon layer thickness, illumination-wavelength and -power density, and the number of illumination cycles. However, thermal back-relaxation (sometimes for many hours) always regenerated the original state, thus indicating the full reversibility of the photoisomerization-induced optical and structural changes in these copolymeric systems.

As has been pointed out above, the particular practical importance of waveguide spectroscopy originates from the fact that various modes can be excited at different angles with different polarizations thus giving information about refractive indices along different spacial coordinates. It is therefore possible to evaluate the full indicatrix of the material in addition to the sample's thickness.
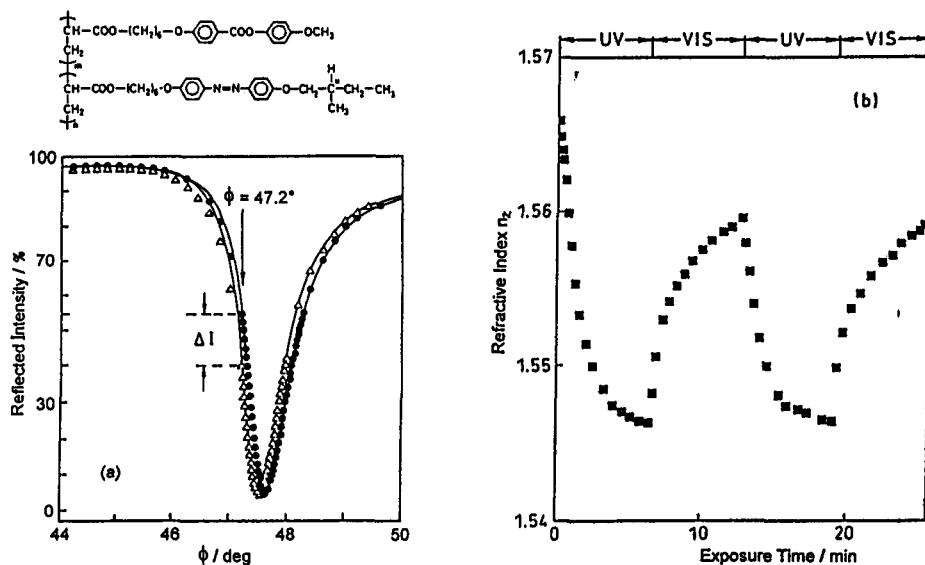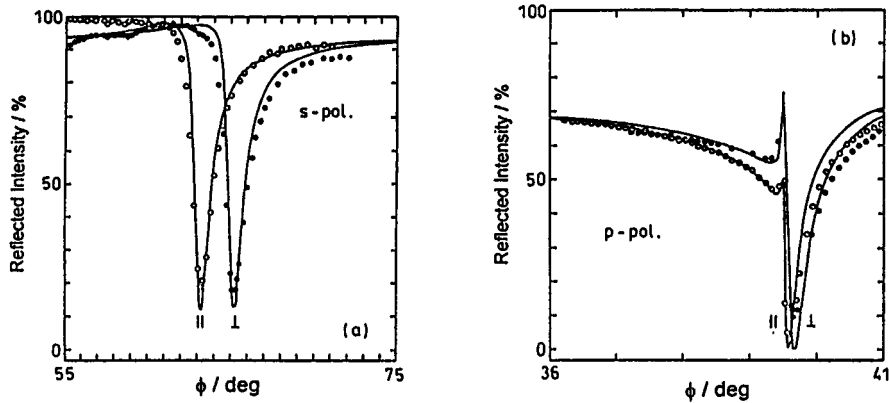

Figure 6

Figure 7

This is exemplified in Fig. 7 for the homopolymer system already introduced in Fig. 5. Forty-seven dipping cycles (with a doublelayer deposited at each cycle) resulted in an LBK multilayer assembly of d = 238 nm, thick enough to carry one waveguide mode for s-polarized excitation (Fig. 7(a)) and one for p-polarized light (Fig. 7(b)) [8]. Upon rotation of the sample in the x,y-plane by 90° these modes were propagating either parallel to the dipping direction of the deposition process (denoted | ||) or perpendicular to it (denoted ⊥ in Fig. 7). In this way, the in-plane anisotropy of the refractive index could be directly visualized, in particular, for s-polarized light because of the propagation properties and hence the coupling conditions for these modes depend only on the in-plane refractive index.

The full curves that describe the experimental data in Fig. 7 are calculated according to Fresnel's formulas with a consistent set of 3 refractive indices: n_z=1.493, $n_{//}$, and $n_{\perp}$ =1.530, and a thickness per monolayer of d_0= 2.52 nm, which coincides with the values obtained from X-ray reflectometry. Note that the difference of the angular position of the s-polarized modes propagating along different directions which amounts to $\Delta\phi$≈2.5 deg. corresponds to a difference of the respective in-plane indices of refraction of only Δn=0.018. Thus, this technique is highly sensitive to monitor even subtle differences or changes in the optical anisotropy of thin polymeric/organic films.

A very interesting aspect of the trans-cis photoisomerization reaction of azobenzene-functionalized polymers concerns their use as command layers in the optical switching of liquid-crystalline display cells.

The command surfaces consist of one to five monomolecular layers of a polymer with azobenzene side chains deposited according to the LBK-technique. When exposed to light of appropriate wavelength the command surfaces undergo a trans↔cis photoisomerization process that induces a reversible change in the liquid-crystal orientation. Such an orientation change of the LC alters the optical properties substantially.
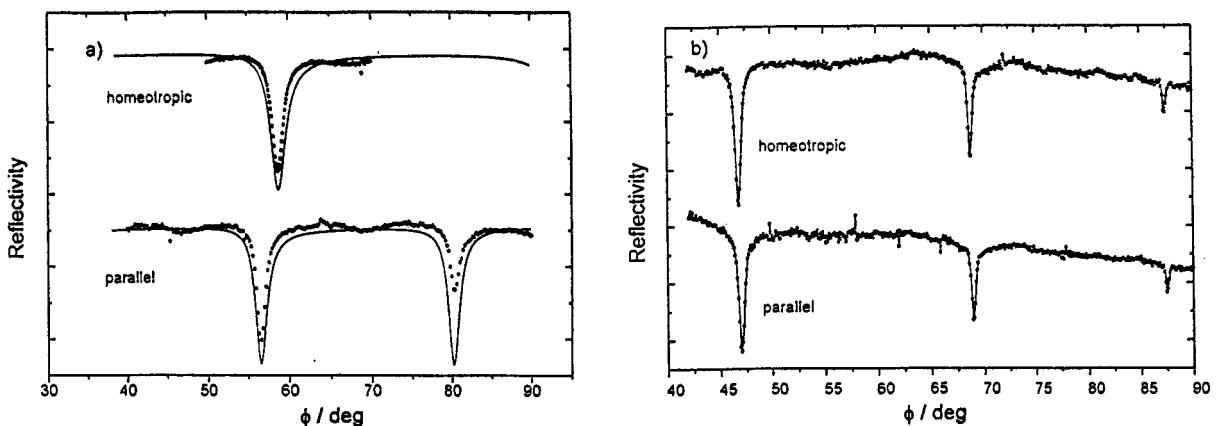

Figure 8

As a first experiment, we measured the reflectivity of the LC cell before and after UV light exposure at a wavelength of λ=360 nm. After irradiating the sample for 10 min, the reflectivity curve was recorded under permanent exposure. While for TM-polarized waveguide modes there is a large difference between the two switching states (shown in Figure 8(a)), for TE polarization (Fig. 8(b)) the reflectivity curve seems to be unaffected.

When comparing the measured reflectivity curves with Fresnel calculations (full curves in Fig. 8), one finds that the experimental data for the refractive indices n_x and n_z are in good agreement with those given by the manufacturer of the LC material for the ordinary (n_0=1.479) and the extraordinary (n_e=1.567) beam. Before UV exposure the calculated value of n_x corresponds to n_0 and that of n_z to n_e. This indicates that the LC molecules are aligned perpendicularly to the command surface (homeotropic). After irradiation, the set of refractive indices changed: now n_x corresponds to n_e and n_z to n_0, indicating that the LC changed its orientation. The LC is now in a parallel alignment with respect to the command layer surface. When exposing the cell to visible light of 450 nm the LC is switched back to the homeotropic state and the reflectivity curve is the same as before UV exposure.

These alignment changes can be cycled many times and show an interesting time behavior and irradiation power dependence. Particularly remarkable is also the interplay between the dipping direction of the command layer deposition and the effect of the polarization of the commanding light [10].

Acknowledgements

References

1)   H. Raether, in: Physics of Thin Films, edited by G. Hass, M.H. Francombe, and R.W. Hoffmann (Academic, New York, 1977) Vol. 9, pp. 145-261.

2)   E. Kretschmann, Opt. Commun. 6 (1972) 185.

3)   W. Knoll, MRS Bulletin XVI (1991) 29.

4)   P.K. Tien, Rev. Mod. Physics 49 (1969) 361.

5)   M. Sawodny, J. Stumpe, and W. Knoll, J. Appl. Phys. 69 (1991) 1927.

6)   R.D. Miller and J. Michl, Chem. Rev. 89 (1989) 1359.

7)   F. Embs, G. Wegner, C.G. Miller, D. Neher, P. Albouy, R.D. Miller, and W. Schrepp, Macromolecules 24 (1991) 5068.

8)   M. Sawodny, A. Schmidt, M. Stamm, W. Knoll, C. Urban, and H. Ringsdorf, Polymers Adv. Technol. 2 (1991) 127.

9)   A. Schmidt, M. Sawodny, W. Knoll, C. Urban, H. Ringsdorf, R.C. Ahuja, and D. Möbius, Acta Polymerica 45 (1994) 217.

10)   H. Knobloch, H. Orendi, M. Büchel, T. Seki, S. Ito, and W. Knoll, J. Appl. Phys. 00 (1994) 000.